Iridanonaborane Chemistry. Some Reactions of *arachno*-4-Iridanonaboranes: Nuclear Magnetic Resonance Investigations and the Molecular Structure of the *nido* Nine-vertex Species [2,2,2-(CO)$(PMe_3)_2$-*nido*-2-IrB_8H_{11}] *

Jonathan Bould, Norman N. Greenwood,* and John D. Kennedy
Department of Inorganic and Structural Chemistry, University of Leeds, Leeds LS2 9JT

arachno-4-Iridanonaboranes may be deprotonated with KH and subsequent reaction with *cis*-$[PtCl_2(PMe_3)_2]$ yields *arachno*-6,9-dimetalladecaboranes such as the compound $[(PMe_3)_2PtB_8H_{10}IrH(PMe_3)_2(CO)]$ which has been characterized by detailed multi-element single- and multiple-resonance n.m.r. spectroscopy. Mild thermolysis or u.v. photolysis of the *arachno*-4-iridanonaboranes yields the corresponding *nido*-2-iridanonaboranes which have been characterized by a single-crystal *X*-ray diffraction analysis of $[(CO)(PMe_3)_2IrB_8H_{11}]$; these are the first *nido* nine-vertex metallaboranes to be structurally characterized and the IrB_8 cluster is based on that of a bicapped Archimedean square antiprism with an equatorial five-connected vertex missing, and with the Ir atom on the open face. The *arachno* ⟶ *nido*-transformation by dihydrogen loss is quantitative and has been followed by ^{11}B n.m.r. spectroscopy. The kinetics are first order with $\Delta H^{\ddagger}$ = *ca.* 130 kJ mol^{-1} and $\Delta S^{\ddagger}$ = *ca.* 30 J K^{-1} mol^{-1} for the compounds studied.

We have reported recently the preparation and characterization of a series of *arachno* nine-vertex iridaboranes typified by [1-Cl-4,4,4,4-(CO)H$(PMe_3)_2$-*arachno*-4-IrB_8H_{11}] (1).[1] The isolation of this and other *arachno*-iridanonaboranes in modest yield permits their further chemical investigation. Accordingly, we here describe two interesting reactions undergone by these species, specifically their deprotonation followed by treatment with *cis*-$[PtCl_2(PMe_3)_2]$ to give bimetallic *arachno* ten-vertex metallaboranes, and their quantitative thermolysis to give *nido* nine-vertex iridaboranes. These last compounds are novel and we describe and report details of the characterization of a representative example by single-crystal *X*-ray diffraction analysis. The work forms part of a systematic survey of borane-to-metal interactions using the heavier transition elements such as platinum,[2-15,‡] iridium,[14-24,‡] osmium,[25] and gold [26,‡] as model metal centres. Some details of the single-crystal *X*-ray diffraction involved in the present work have been reported previously.[27]

Results and Discussion

It is known that the reaction of the *arachno*-platinanonaborane $[(PMe_2Ph)_2PtB_8H_{12}]$ with non-nucleophilic bases such as KH results in its deprotonation, and that its subsequent reaction with *cis*-$[PtCl_2(PMe_2Ph)_2]$ then readily yields the diplatinadecaborane species $[(PMe_2Ph)_4Pt_2B_8H_{10}]$, equation (i).[7] We have

$$[(PMe_2Ph)_2PtB_8H_{12}] + 2KH + [PtCl_2(PMe_2Ph)_2] \longrightarrow [(PMe_2Ph)_4Pt_2B_8H_{10}] + 2KCl + H_2 \quad (i)$$

now found that an exactly analogous reaction also occurs with the more recently reported [1] *arachno*-iridanonaborane, $[(CO)(PMe_3)_2HIrB_8H_{12}]$ (2), with a similar stoicheiometry: equation (ii). The product, a colourless, air-stable crystalline

$$[(CO)(PMe_3)_2HIrB_8H_{12}] + 2KH + [PtCl_2(PMe_3)_2] \longrightarrow [(CO)(PMe_3)_2HIrB_8H_{10}Pt(PMe_3)_2] + 2KCl + H_2 \quad (ii)$$

solid (3), was isolated in *ca.* 12% yield when the reaction was carried out on a scale of 0.17 mmol. Although the compound was thermally quite stable, and exhibited no decomposition when heated to 135 °C in solution, single crystals decomposed on exposure to the *X*-ray beam of a diffractometer. However, the structure was readily deduced from the results of detailed ^{31}P, ^{11}B, and ^1H single- and multiple-resonance n.m.r. spectroscopy. Borane cluster ^{11}B and ^1H n.m.r. shielding and coupling constant data are summarized in Table 1, and ^1H and ^{31}P data associated with the metal environments are in Table 2; a low-temperature ^{31}P-{^1H(broad-band noise)} spectrum [3] is illustrated in Figure 1.

The similarity of the ^{11}B shieldings with those of the known [7] diplatinadecaborane $[(PMe_2Ph)_4Pt_2B_8H_{10}]$ together with the known [1,7] differential effects of platinum and iridium centres on the shieldings within *arachno* eight-boron clusters readily identify the product as an *arachno*-6,9-platinairidadecaborane cluster species, and also assign the boron resonances. These last were additionally confirmed by the observation of satellites arising from $^1J(^{195}Pt-^{11}B)$ for the B(2), B(7), and B(11) positions. The eight B–H terminal hydrogen atoms and two bridging hydrogen atoms H(7,8) and H(10,11) were readily established by selective ^1H-{^{11}B} spectroscopy,[6,7] and these results were entirely consistent with expected behaviour. That the resonances for the (1)/(3), (7)/(10), and (8)/(9) positions were not pairwise degenerate shows that one or both of the metal centres is asymmetric with respect to the formal mirror plane of the $IrPtB_8$ cluster. That the asymmetry arises from the iridium centre follows from consideration of the ^1H and ^{31}P n.m.r. data (Table 2 and Figure 1), which show that the stereochemistry of the iridium centre is the same as that [1] in the starting *arachno*-iridanonaborane, [*asym*-4,4,4,4-(CO)-*endo*-H-*cis*-$(PMe_3)_2$-4-IrB_8H_{12}] (2). The structure of the dimetalladecaborane thus established, *viz.* [6,6-$(PMe_3)_2$-*asym*-9,9,9,9-(CO)-*endo*-H-*cis*-$(PMe_3)_2$-*arachno*-6,9-platinairidadecaborane], is represented in Figure 2.

* 2-Carbonyl-2,2-bis(trimethylphosphine)-*nido*-2-iridanonaborane.

Supplementary data available (No. SUP 56035, 20 pp.): structure factors, thermal parameters. See Instructions for Authors, *J. Chem. Soc., Dalton Trans.*, 1984, Issue 1, pp. xvii—xix.

‡ Most recent work on related compounds: ref. 11, reactions of $(Me_2S)_2B_{10}H_{12}$ with platinum complexes; ref. 12, preparation, synthesis, and n.m.r. studies of halogenated *nido*-platinaundecaboranes; ref. 13, reactions of $B_{10}H_{13}OH$ and $(B_{10}H_{13})_2O$ with platinum complexes; ref. 24, structural studies of $[(CO)(PPh_3)_2HIrB_3H_7]$; ref. 26, structures and n.m.r. study of *arachno*-AuB_8 and -Au_2B_8 cluster compounds.

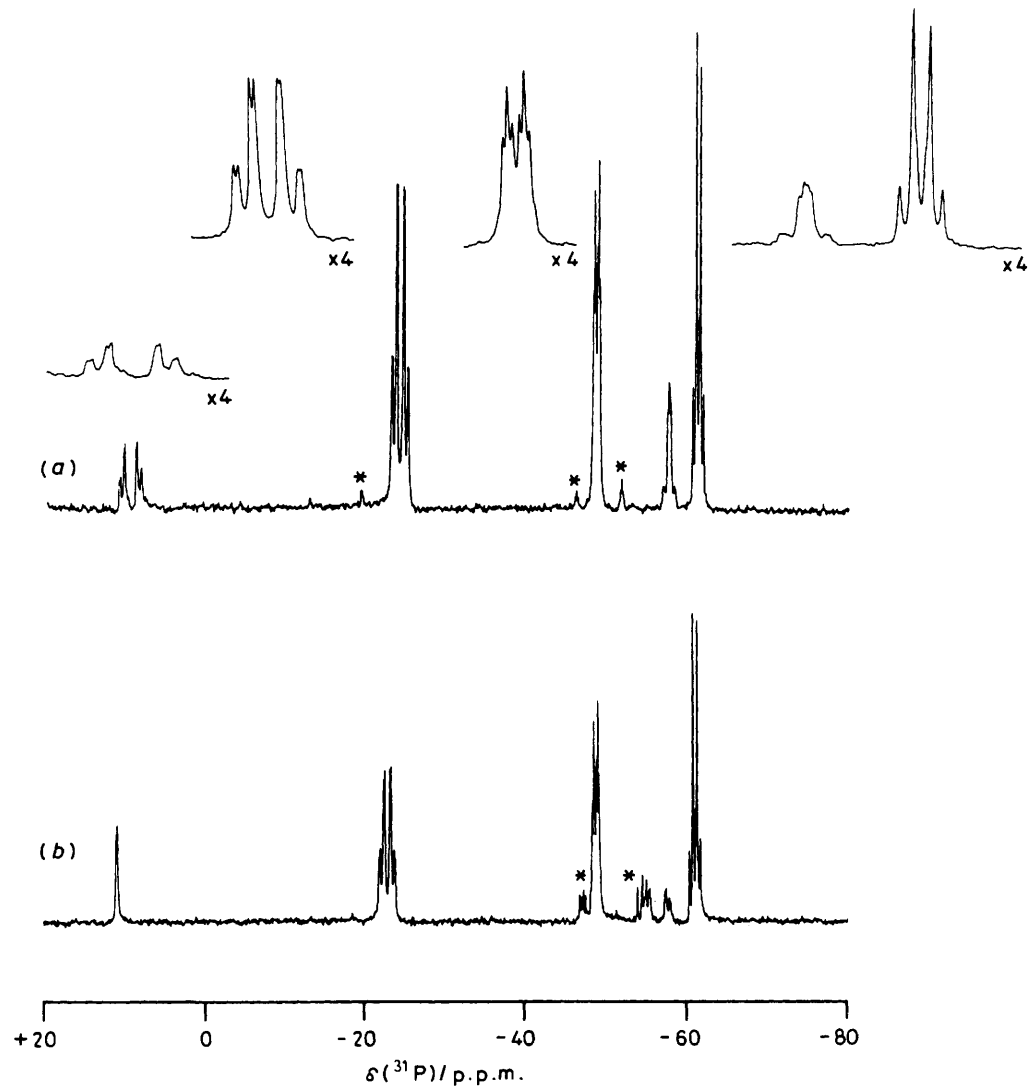

Figure 1. Phosphorus-31-{^{1}H(broad-band noise)} n.m.r. spectra (40.25 MHz; CD_2Cl_2 solution) of (3) at (*a*) −88 and (*b*) −50 °C. * Signifies impurity

Although dimetalladecaborane species are now well established [7,13,28-30] this is the first one reported that has metals from two different groups of the periodic table. An interesting consequence of this in this case is that the two metal-to-borane bonding modes may differ in important detail. This is established from the similarity of the n.m.r. properties, for the atoms about the different metal centres, with those of the previously reported species $[(PMe_2Ph)_2PtB_8H_{12}]$,[7] $[(PMe_2Ph)_4Pt_2B_8H_{10}]$,[7] and $[(CO)(PMe_3)_2HIrB_8H_{11}Cl]$ (1),[1] for which *X*-ray molecular structures have been determined and the bonding modes discussed in some detail.[1,7] In accord with these parallels the borane-to-metal bonding at the iridium centre is probably best regarded at present as occurring predominantly *via* two two-electron bonds. That to the platinum atom is more ambiguously defined at present,[7] but contributions from structures with three two-electron bonds are probably quite important. In these terms semi-localized valence-bond structures such as (I) (Figure 3) may therefore be proposed to describe major contributions to the cluster electronic structure of the dimetallic species (3); these are equivalent to that for a hypothetical *arachno* binary boron hydride species $[B_{10}H_{13}]^{3-}$ of 2551 *styx* bonding topology depicted in Figure 3, structure (II). Within this general formalism, the valency states of the two metal atoms may be regarded essentially as iridium(III) and platinum(IV), although in the compound itself the bonding at the latter atom will retain significant platinum(II) character.

There are some further points arising from the ^{31}P n.m.r. data of Tables 1 and 2 that merit further comment. First, there is a noticeable variation with temperature both in the chemical shifts and in the coupling constants, and at 40 MHz the positions of a number of lines in the spectrum are fortuitously such that this leads to marked changes in the appearance of the ^{31}P-{^{1}H(broad-band noise)} spectra. These types of temperature variation have been little studied,[3,31] but the variations in the observed couplings $^1J(^{195}Pt-^{31}P)$ of *ca.* +1.2 and −0.4 Hz K^{-1}, for example, are significantly larger than those previously observed in phosphine ligands in platinaborane systems.[3] Presumably in the present case Ir–P, Pt–P, and P–C rotamer populations in the sterically rather crowded area above the metallaborane cluster open face will be of significance in this respect. A second point is the observation of splittings in the phosphorus spectrum due to the longer-range four- and five-bond interactions arising from *trans*-cluster coupling paths. Similar couplings have been noted elsewhere in species such as $[(PMe_2Ph)_4Pt_2B_8H_{10}]$,[7] $[(PMe_2-$

Table 1. Boron-11 and proton n.m.r. data for the borane cluster of $[(CO)(PMe_3)_4HIrPtB_8H_{10}]$ (3) in $CDCl_3$ solution at +21 °C

Assignment of position	$\delta(^{11}B)$ [a]/p.p.m.	$\delta(^1H)$ [b]/p.p.m.	$^1J(^{11}B-^1H)$/Hz
(2)	+25.2 [c]	+4.64 [c]	*ca.* 120
(4)	+15.9	+4.19 [d]	*ca.* 130
(5), (7)	−4.0 [e]	+2.54 [f]	[g]
	−5.0 [e]	+2.64 [f]	[g]
(8), (10)	−9.5	+2.49	[g]
	−12.3	+2.46	[g]
(1), (3)	−27.1	+1.33 [f]	*ca.* 140
	−28.9	+1.37 [f]	*ca.* 140
(5)/(10) (bridge)	—	−2.95 [h]	[g]
(7)/(8) (bridge)	—	−3.27 [i]	[g]
(9) (Ir terminal)	—	−13.50 [j]	—

[a] To high frequency (low field) of $BF_3{\cdot}OEt_2$ in $CDCl_3$ [Ξ = 32 083 971 Hz], ±0.5 p.p.m. [b] To high frequency (low field) of $SiMe_4$, ±0.05 p.p.m. [c] $^1J(^{195}Pt-^{11}B) = 280 \pm 30$ and $^2J(^{195}Pt-^1H) = 20 \pm 10$ Hz; signs opposite by selective $^1H-\{^{11}B\}$ spectroscopy. [d] $^3J(^{31}P_{ax}-Ir-B-^1H)(cis) = 39 \pm 2$ Hz; no differential effects in selective $^1H\{^{11}B\}$ experiments indicating that $^2J(^{31}P-Ir-^{11}B)(cis)$ is small. [e] $^1J(^{195}Pt-^{11}B)$ = *ca.* 280 Hz. [f] Any ^{195}Pt 'satellite' structure in ^1H spectrum obscured by overlapping resonances at 100 MHz. [g] Not measured: resolution insufficient. [h] $^2(J^{195}Pt-^1H) = 35 \pm 15$ Hz. [i] $^2J(^{195}Pt-^1H) = 40 \pm 10$ Hz. [j] Doublet of doublets with $^2J(^{31}P_{ax}-^1H)(trans) = 142 \pm 2$ and $^2J(^{31}P_{eq}-^1H)(cis) = 18 \pm 2$ Hz, with additional broadening arising from $^4J(^1H-C-P_{ax}-Ir-^1H)(transoid) = 0.9 \pm 0.2$ Hz.

$Ph)_4PdPtB_8H_{10}]$,[13] and $[(PMe_2Ph)_4HPt_3B_{12}H_{17}]$, [13] and in the present case the incidence of comparable magnitudes for couplings $^5J(^{31}P-^{31}P)$ *cisoid* and *transoid* to the equatorial trimethylphosphine ligand tends to endorse the supposition previously made[7] that the two analogous couplings in $[(PMe_2Ph)_4Pt_2B_8H_{10}]$ also have similar magnitudes and therefore the same sign. The absence of a measurable coupling $^5J(^{31}P-^{31}P)$ to the axial trimethylphosphine ligand emphasizes conclusions made elsewhere[13] for $[(PMe_2Ph)_4HPt_3B_{12}H_{17}]$ that these couplings have a critical dependence on the stereochemical path; this is not unexpected.

The second aspect of metalloborane chemistry associated with the *arachno*-4-iridanonaboranes such as (1) and (2) stems from observations made initially whilst determining the melting points of these species. Straightforward heating of these compounds results in their decomposition by loss of dihydrogen to yield corresponding *nido*-iridanonaboranes, exemplified in equation (iii) for $[(CO)(PMe_3)_2HIrB_8H_{12}]$ (2). The reaction may be effected very rapidly by immersion of a vessel containing the *arachno* species in an oil bath maintained at +180 °C, followed by chromatographic separation to yield the *nido* product. Under these conditions we found typical isolable yields of *ca.* 60% when the reaction was conducted on a scale of 0.02 mmol. Alternatively the conversion may be effected quantitatively, but more slowly, in solution at lower temperatures as described in more detail below. The reactions occur with similar facility for both (2) and the chloro-species (1); insufficient quantities of the third known[1] *arachno*-4-iridanonaborane, $[(PMe_3)_3HIrB_8H_{12}]$, were available for it to be examined thoroughly for similar behaviour, although the indications were that the reaction occurred easily for this species also.

$$[(CO)(PMe_3)_2HIrB_8H_{12}] \longrightarrow \underset{(2)}{} [(CO)(PMe_3)_2IrB_8H_{11}] + H_2 \quad \text{(iii)}$$
(4)

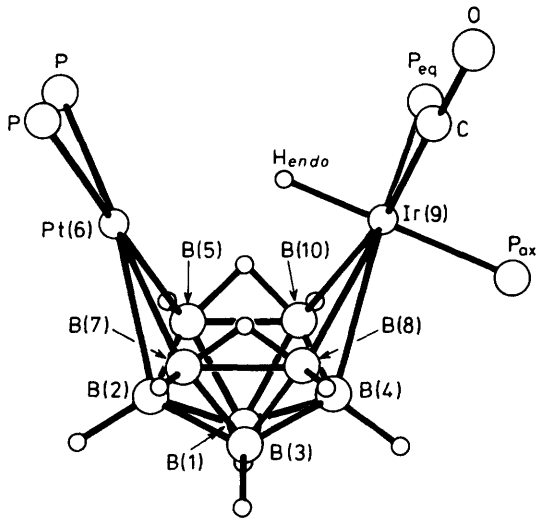

Figure 2. Representation of the proposed molecular structure of *arachno*-$[(PMe_3)_2PtB_8H_{10}IrH(PMe_3)_2(CO)]$ (3). N.m.r. evidence suggests that the bonding and stereochemistry about Pt(6) and Ir(9) are essentially the same as about the metal atoms in $[(PMe_2Ph)_2PtB_8H_{12}]$[7] and $[(CO)(PMe_3)_2HIrB_8H_{11}Cl]$[1] respectively (see Figure 3)

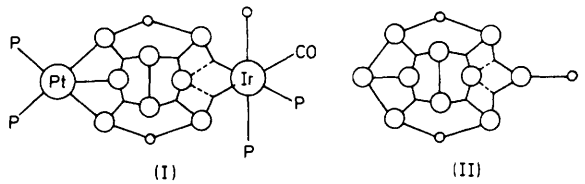

Figure 3. Semi-localized valence-bond structure (I) to illustrate the basis of the differences in borane-to-platinum and borane-to-iridium bonding contributions for *arachno*-$[(PMe_3)_2PtB_8H_{10}IrH(PMe_3)_2(CO)]$ (3). The analogous *arachno* binary species $[B_{10}H_{13}]^-$ would have 2551 *styx* topology as in (II). In each case a number of additional contributory canonical forms may be written (see refs. 1, 7, and 26), and the borane-to-platinum bonding in (I) will also have contributions from a two-orbital binding mode similar to that depicted for the iridium–borane interaction

The products, $[(CO)(PMe_3)_2IrB_8H_{11}]$ (4) and $[(CO)(PMe_3)_2IrB_8H_{10}Cl]$ (5), are the first examples of *nido* nine-vertex metallaboranes to be described; they are very pale yellow air-stable crystalline solids, and were characterized by single- and multiple-resonance n.m.r. spectroscopy together with single-crystal *X*-ray diffraction analysis on the non-chlorinated compound (4), as reported previously[27] in a preliminary communication. An ORTEP drawing of the molecular structure of (4) is given in Figure 4, and selected interatomic distances and angles between interatomic vectors in Tables 3 and 4. N.m.r. data for both the new *nido* species (4) and (5) are in Tables 5 and 6.

The molecular structure of (4) is based on an IrB_8 nine-vertex *nido* structure with eleven closed triangular faces and one five-vertex open face, corresponding to a bicapped square antiprism with one equatorial (five-connected) vertex missing. The metal atom occupies a position on the open face adjacent to the missing position, but on the second four-atom equatorial belt. The gross geometry is therefore similar to that generally accepted for the *nido*-$[B_9H_{12}]^-$ anion, *i.e.* similar to that found[32] for the carborane analogue $B_7C_2H_9Me_2$, but it is in contrast to that found[33] for the *nido*-metalladicarbaborane $[(PEt_3)_2PtC_2B_6H_8Me_2]$. (This last compound contains a

Table 2. Phosphorus-31 [a] and proton [b] n.m.r. data for the metal atom environment in $[(PMe_3)_2PtB_8H_{10}IrH(PMe_3)_2(CO)]$ (3) [c,d]

(*i*) At the platinum atom				
$\delta[^{31}P(Pt)]$	−24.6 (A)	−26.0 (B)	−22.6 (A) [e]	−23.9 (B) [e]
$^1J(^{195}Pt-^{31}P)$	2 620 ± 5 (A)	2 670 ± 5 (B)	2 608 (A) [e]	2 704 (B) [e]
$^5J[^{31}P(Pt)-^{31}P_{eq}(Ir)]$	6 ± 1(A)	4 ± 1 (B)	5.5 ± 1 (mean of A & B) [e]	
$^2J(^{31}P_A-^{31}P_B)$	22 ± 1	22 ± 1	22 ± 1 [e]	22 ± 1
$\delta[^1H(MeP)]$	+1.60 (C) [f]	+1.61 (D) [f]		
$^3J[^{195}Pt-^1H(MeP)]$	24.5 ± 0.2 (C) [f]	25.3 ± 0.2 (D) [f]		
$^2J[^{31}P-^1H(MeP)]$	8.0 ± 0.5 (C) [f]	8.0 ± 0.5 (D) [f]		
(*ii*) At the iridium atom [g]				
$\delta[^{31}P(Ir)]$	−49.3 (eq)	−61.6 (ax)	−48.6 (eq) [e]	−60.7 (eq) [e]
$^4J(^{195}Pt-^{31}P)$	47 ± 2 (eq)	31 ± 1 (ax)		
$^5J[^{31}P(Pt)-^{31}P(Ir)]$ (mean)	5 ± 1 (eq)	0 ± 1 (ax)	5.5 ± 1 (eq) [e]	*ca.* 0 (ax) [e]
$^2J(^{31}P_{ax}-^{31}P_{ax})$	21 ± 1	21 ± 1	21 ± 1 [e]	
$\delta[^1H(MeP)]$	1.70 (eq)	1.44 (ax)		
$^2J(^{31}P-^1H)$	9.5 ± 0.5 (eq)	8.0 ± 0.5 (ax)		
$^4J[^1H-C-P-Ir-^1H(9)]$	*ca.* 0 (eq)	0.9 ± 0.2 (ax) [h]		
$^3J[^{31}P-Ir-B(4)-^1H(4)]$	*ca.* 0 (eq)	39 ± 4 (ax)		
$^2J[^{31}P-Ir-^1H(9)]$	18 ± 2 (eq) (*cis*) [i]	142 ± 2 (ax) (*trans*) [i]		

[a] CD_2Cl_2 solution at −88 °C. [b] CD_2Cl_2 solution at +21 °C. [c] $\delta(^{31}P)$ in p.p.m. (±0.5) to high frequency (low field) of 85% H_3PO_4 (Ξ = 40 480 730 Hz). $\delta(^1H)$ in p.p.m. (±0.05) to high frequency (low field) of $SiMe_4$. *J* values are in Hz. [d] Designations A and B serve only to distinguish the two chemically different PMe_3 groups. [e] CD_2Cl_2 at −60 °C. [f] Designations C and D serve only to distinguish the two chemically different PMe_3 groups; any AB/CD correspondence has not been established. [g] Designations eq and ax for the PMe_3 groups correspond to those in the structure shown in Figure 2. [h] Confirmed by selective $^1H-\{^1H\}$ spectroscopy. [i] Assigned by selective $^1H-\{^{31}P\}$ spectroscopy.

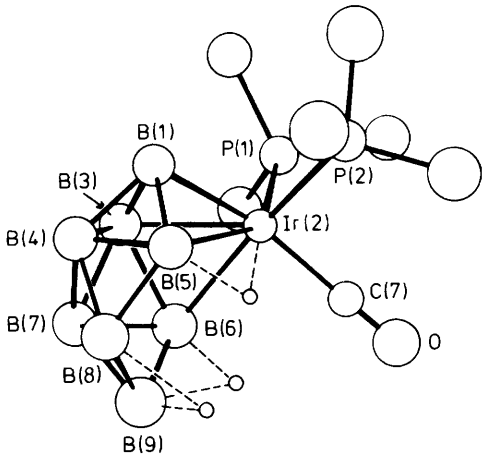

Figure 4. The molecular structure of *nido*-$[(CO)(PMe_3)_2IrB_8H_{11}]$ (4). Hydrogen atoms were not refined, but n.m.r. spectroscopy (Table 5) shows that there is an *exo*-terminal hydrogen atom associated with each boron atom, and that there are bridging hydrogen atoms probably associated with B(6)B(9) and B(8)B(9) as shown; peaks corresponding to these ten hydrogen atoms appeared on final difference maps. In addition the Ir−H · · · B(5) bridging hydrogen-atom stereochemistry as depicted was also apparent from n.m.r. experiments; this is believed to have substantial Ir−H(*endo*) terminal character, and it may be noted that the Ir−B(5) distance is long at *ca.* 250 pm

square four-membered open face which may be obtained by connecting the 2-position with the 9-position in the structure shown in Figure 4.)

Hydrogen atoms were not located, but selective $^1H-\{^{11}B\}$ n.m.r. spectroscopy showed that each boron atom had one terminal hydrogen atom bonded to it, and that there were additionally two B−H−B bridging hydrogen atoms, presumably associated with B(6)B(9) and B(8)B(9); peaks corresponding to these positions appeared in the final difference maps. Selective $^1H-\{^{11}B\}$ spectroscopy also revealed a high-field proton resonance associated with just one boron atom [*i.e.* $\delta(^1H) = -14.5$ associated with $\delta(^{11}B) = -39.9$ p.p.m.] (Table 5). This we ascribe to the Ir(2)−H−B(5) bridging hydrogen since it exhibits a large splitting of *ca.* 62 Hz consistent with [20] a *trans* coupling $^2J(^{31}P-Ir-^1H)$ to the phosphorus P(1), although it should be pointed out that the *X*-ray data obtained were insufficient to establish this particular H-atom position in the difference maps. However, compound (4) is reasonably formulated as $[(CO)(PMe_3)_2IrB_8H_{11}]$, which is consistent also with the mass spectrum of the species which had a molecular ion corresponding to this formula weight. Interestingly the mass spectrum was identical to that [1] obtained from the *arachno* precursor (2), emphasizing the facility of H_2 loss in this system.

Table 3. Selected interatomic distances (pm) for [2,2,2-(CO)$(PMe_3)_2$-*nido*-2-IrB_8H_{11}] (4), with estimated standard deviations in parentheses

(*i*) From the iridium atom			
Ir(2)−P(1)	232.0(2)	Ir(2)−B(1)	218.5(8)
Ir(2)−P(2)	235.9(2)	Ir(2)−B(3)	230.4(7)
Ir(2)−C(7)	191.2(8)	Ir(2)−B(5)	250.0(6)
		Ir(2)−B(6)	233.0(10)
(*ii*) Boron–boron			
B(1)−B(3)	176.5(11)	B(4)−B(8)	183.8(14)
B(1)−B(4)	168.6(12)	B(5)−B(8)	187.7(12)
B(1)−B(5)	177.3(13)	B(6)−B(7)	177.0(14)
B(3)−B(4)	178.4(12)	B(6)−B(9)	178.4(15)
B(3)−B(6)	184.5(12)	B(7)−B(8)	183.4(13)
B(3)−B(7)	180.4(12)	B(7)−B(9)	175.4(16)
B(4)−B(5)	181.9(12)	B(8)−B(9)	184.2(15)
B(4)−B(7)	182.0(12)		
(*iii*) Other			
C(7)−O(7)	115.8(9)		
P(1)−C(methyl)	179.9(7)—180.4(8)		
P(2)−C(methyl)	177.9(9)—178.5(9)		

Table 4. Selected angles (°) between interatomic vectors for $[(CO)(PMe_3)_2IrB_8H_{11}]$ (4) with estimated standard deviations in parentheses

(*i*) At the iridium atom

P(1)–Ir(2)–P(2)	96.3(1)	P(1)–Ir(2)–B(6)	95.4(3)	P(2)–Ir(2)–C(7)	95.3(2)	B(1)–Ir(2)–B(3)	46.2(3)
P(1)–Ir(2)–C(7)	88.7(2)	C(7)–Ir(2)–B(1)	167.4(3)	P(2)–Ir(2)–B(1)	89.4(2)	B(1)–Ir(2)–B(5)	43.8(3)
P(1)–Ir(2)–B(1)	102.4(2)	C(7)–Ir(2)–B(3)	130.5(3)	P(2)–Ir(2)–B(3)	134.2(2)	B(1)–Ir(2)–B(6)	88.0(3)
P(1)–Ir(2)–B(3)	85.4(2)	C(7)–Ir(2)–B(5)	124.5(3)	P(2)–Ir(2)–B(5)	88.3(2)	B(3)–Ir(2)–B(5)	68.1(3)
P(1)–Ir(2)–B(5)	146.1(2)	C(7)–Ir(2)–B(6)	85.0(3)	P(2)–Ir(2)–B(6)	168.3(3)	B(3)–Ir(2)–B(6)	46.8(3)
						B(5)–Ir(2)–B(6)	81.9(3)

(*ii*) Iridium–boron–boron

Ir(2)–B(1)–B(3)	70.4(4)	Ir(2)–B(3)–B(4)	101.4(4)	Ir(2)–B(5)–B(1)	58.6(3)	Ir(2)–B(6)–B(3)	65.8(4)
Ir(2)–B(1)–B(4)	109.9(5)	Ir(2)–B(3)–B(6)	67.3(4)	Ir(2)–B(5)–B(4)	93.5(4)	Ir(2)–B(6)–B(7)	110.7(5)
Ir(2)–B(1)–B(5)	77.6(4)	Ir(2)–B(3)–B(7)	110.5(5)	Ir(2)–B(5)–B(8)	106.8(5)	Ir(2)–B(6)–B(9)	113.7(6)
Ir(2)–B(3)–B(1)	63.3(3)						

(*iii*) Other

B(1)–B(3)–B(6)	120.7(6)	B(3)–B(6)–B(9)	112.4(7)	B(6)–B(9)–B(8)	100.4(7)
B(1)–B(5)–B(8)	111.5(6)	Ir(2)–C(7)–O(7)	176.1(6)	Ir(2)–P(1)–C(methyl)	105.6(4)—115.5(3)
B(3)–B(1)–B(5)	99.2(6)	B(5)–B(8)–B(9)	113.4(6)	Ir(2)–P(2)–C(methyl)	114.0(3)—119.2(3)

Table 5. Boron-11 and proton n.m.r. parameters of the metallaborane clusters of $[(CO)(PMe_3)_2IrB_8H_{11}]$ (4), $[(CO)(PMe_3)_2IrB_8H_{10}Cl]$ (5), and $[(PMe_3)_3IrB_8H_{11}]$ (6)

Tentative positional assignment	Compound (4) [a]		Compound (5) [a]		Compound (6) [b]
	δ(^{11}B) [c]/p.p.m.	δ(^{1}H) [d]/p.p.m.	δ(^{11}B) [c]/p.p.m.	δ(^{1}H) [d]/p.p.m.	δ(^{11}B) [c]/p.p.m.
—	+23.1	+5.04	+22.6	+5.06	+26.9
—	+8.8	+4.90	+13.5	+5.32	+10.1
(3)			+1.1	*e*	
—	−5.3	+2.94	−3.5	+3.05	−3.4
two of (6), (8), (9)	−13.6	+1.02	−9.0	+1.50	−15.0
	−14.5	+2.99	−14.2	+3.05	−15.0
(3)	−15.3	+0.83 [f]			−16.2
(5)	−39.9	−0.51, −14.50 [g]	−40.8	−0.87, −14.60 [h]	−40.5
—	−52.5	−1.48	−47.4	−1.19	−49.8
(6)/(9), (8)/(9) (bridge)	—	−2.10 [i], −2.96 [i]	—	−2.03, [j] −2.50 [j]	

[a] $CDCl_3$ solution at +21 °C. [b] $CD_3C_6D_5$ solution at +105 °C; ^{1}H data not measured. [c] ±0.5 p.p.m. to low field (high frequency) of $BF_3{\cdot}OEt_2$ in $CDCl_3$. [d] ±0.05 p.p.m. to low field (high frequency) of $SiMe_4$. [e] Chlorinated B atom. [f] No coupling $^3J(^{31}P–Ir–B–^1H)$ apparent (in contrast to IrB_8 species in ref. 1 and Ir_2B_4 species in ref. 21). [g] $^2J(^{31}P–^1H) = 62$ Hz; confirmed by ^1H-{^{31}P} experiments. Compare to similar coupling of 52 Hz in $[(PMe_3)_2HIrB_9H_{13}]$ (ref. 20). [h] $^2J(^{31}P–^1H) = 49$ Hz; confirmed by ^1H-{^{31}P} experiments. [i] Apparently selectively sharpened when δ(^{11}B) = −13.6 to −15.3 p.p.m. selectively irradiated in ^1H-{^{11}B} experiments. [j] Apparently selectively sharpened when δ(^{11}B) = −9.0 and −14.2 p.p.m. selectively irradiated in ^1H-{^{11}B} experiments.

Table 6. Phosphorus-31 [a] and proton [b] n.m.r. data (*J* values in Hz) for the metal environment in $[(CO)(PMe_3)_2IrB_8H_{11}]$ (4) and $[(CO)(PMe_3)_2IrB_8H_{10}Cl]$ (5); $CDCl_3$ solutions

	Compound (4)	Compound (5)
δ(^{31}P) [c,d]	−39.5 (B), −50.5 (A)	−35.1, −51.1
$^2J(^{31}P–^{31}P)$	19 ± 1	19 ± 1
δ[^{1}H(MeP)] [d,e]	+1.76 (A), +1.73 (B)	+1.92 (A), +1.80 (B)
$^2J[^{31}P–C–^1H(MeP)]$ [d]	9.5 ± 0.4 (A), 10.5 ± 0.4 (B)	9.5 ± 0.4 (A), 10.5 ± 0.4 (B)
δ[^{1}H(Ir–H–B)] [e]	−14.5	−14.6
$^2J(^{31}P–Ir–^1H)$(*trans*) [f]	62 ± 1	49 ± 1

[a] At −50 °C. [b] At +21 °C. [c] In p.p.m. (±0.5) to high frequency (low field) of 85% H_3PO_4 (Ξ = 40 480 730 Hz). [d] A and B distinguish the two chemically different PMe_3 groups in each case; ^{31}P and ^{1}H resonances correlated by selective ^1H-{^{31}P} spectroscopy. [e] In p.p.m. (±0.05) to high frequency (low field) of $SiMe_4$. [f] Confirmed by ^1H-{^{31}P} spectroscopy.

The identity of the corresponding chloro-derivative $[(CO)(PMe_3)_2IrB_8H_{10}Cl]$ (5) readily follows from the comparative n.m.r. behaviour with that of the non-chloro compound (4), and it seems reasonable (see below) to ascribe the site of the chloro-substituent to B(3); unfortunately at present it is not possible to assign the ^{11}B spectra of these species with any degree of certainty. In both the chloro-compound (5) and the non-chloro-compound (4) the ligand geometry about the metal atom appears to be essentially identical, which is of interest since this geometry differs between the two *arachno* precursor compounds (1) and (2).

Within the cluster, the boron–boron distances are within normal ranges, although distances to B(1) are towards the shorter end of these. Of these, the rather short distance B(1)–B(4) of 168.6(12) pm has parallels in the similar distance [34] of *ca.* 172 pm in the *closo*-$[B_{10}H_{10}]^{2-}$ anion. Distances from the iridium atom to the phosphine and carbonyl ligands are also within normal ranges and the iridium–boron distances of 230.4(7) and 233.0(10) pm to B(3) and B(6) respectively may be compared to the similar distances from Ir(4) to B(1), B(5), and B(9) in the *arachno* precursor (2) [1] of 226.1(10)—229.1(8) pm. Again, however, the distance to B(1) is much shorter at 218.5(8) pm which may imply more two-centre character for the Ir(2)–B(1) linkage. By contrast, the hydrogen-bridge distance Ir(2)–B(5) is markedly longer, at 250.0(6) pm, than the direct Ir–B distances, and also longer than the ostensibly analogous Ir–H–B bridged distances of 225—229 pm in

Table 7. Proton and boron-11 chemical shift data for $[NEt_4][B_9H_{12}]$ in CD_2Cl_2 solution, with relative intensities in parentheses

$\delta(^{11}B)$ [a] (+21 °C)	$\delta(^1H)$ [b] (−80 °C)		$\delta(^1H)$ [b,c] (21 °C)	
−10.0 (3)	+2.64 (2) [d], +1.63 (1)	−2.98 (2) [e]	+2.69 (2), +1.74 (4)	−4.31 (3)
−14.4 (3)	+1.63 (3)			
−34.2 (2)	+0.63 (2), −7.22 (1)		+0.75 (2)	
−52.0 (1)	−1.00 (1)	−1.00 (1)	−0.91 (1)	

[a] In p.p.m. (±1.5) to high frequency (low field) of $BF_3{\cdot}OEt_2$ in $CDCl_3$. [b] In p.p.m. (±0.05) to high frequency (low field) of $SiMe_4$; proton resonances correlated with those of boron-11 by selective ^1H-$\{^{11}B\}$ experiments. [c] $\delta(^1H)$ for $[NEt_4]^+$ at +3.10 (quartet) and +1.19 (triplet), $^3J(^1H{-}^1H)$ = 6.8 Hz. [d] Possibly two near-coincident non-equivalent resonances at $\delta(^1H)$ *ca.* +2.62 and +2.66. [e] Possibly two near-coincident non-equivalent resonances at $\delta(^1H)$ *ca.* −2.96 and −3.00 with some selective decoupling with $\nu(^{11}B)$ corresponding to $\delta(^{11}B)$ −10.0 and −14.4 p.p.m.

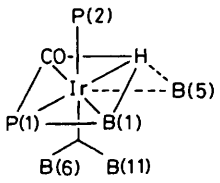

(III)

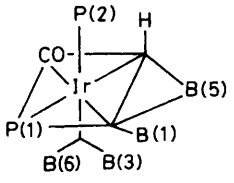

(IV)

previously measured species.[16,20] The proton chemical shift of the Ir–H–B bridging hydrogen atom is at very high field for such a bridging atom, and more in the region (−11 to −17 p.p.m.) previously observed for Ir–H terminal hydrogen atoms in iridaboranes.[1,17,20,22,23,25] These two factors taken together indicate only weak interaction between the B(5) atom and the metal centre as in structure (III) which may be indicative of contributions from an essentially two-orbital rather than three-orbital metal involvement in the cluster bonding. This perhaps arises basically from an incompatability between the iridium(III) octahedral bonding disposition and an angularly more strained involvement such as in (IV). It is interesting to speculate that factors such as this may in fact be related to the instability of the formal parent binary *nido*-borane B_9H_{13} itself.

In any event, the angular dispositions of the ligands about the iridium atom suggest that the bonding geometry about the metal can be regarded as essentially octahedral. In these terms, four of the six bonding electron pairs are directed towards P(1), P(2), the carbonyl group, and the bridging H(2,5) atom; the remaining two will be involved in two two-electron bonds to the three-atom system B(1)B(3)B(6), perhaps in a similar manner to the bonding of Ir(9)B(8)B(4)B(10) in the platinairidadecaborane compound (3) discussed above (Figure 3). However, as also noted above, there may be a large concentration of two-centre character in Ir(2)–B(1) rather than Ir(2)–B(3), and the possibly corresponding absence of a large coupling $^3J(^{31}P{-}Ir{-}B{-}^1H)$ in these *nido* species, as discussed below, also indicates that this particular analogy should not be extended too far.

Considered as a transition metal complex, the compound is a straightforward 'octahedral' 18-electron iridium(III) species, and the borane ligand, subject to the limitations discussed in the previous paragraph, is a pentahapto-tridentate (*i.e.* three electron-pair) *arachno*-octaboranyl ligand, $[B_8H_{11}]^{3-}$, *formally* derived from the triple deprotonation of the known [35] binary

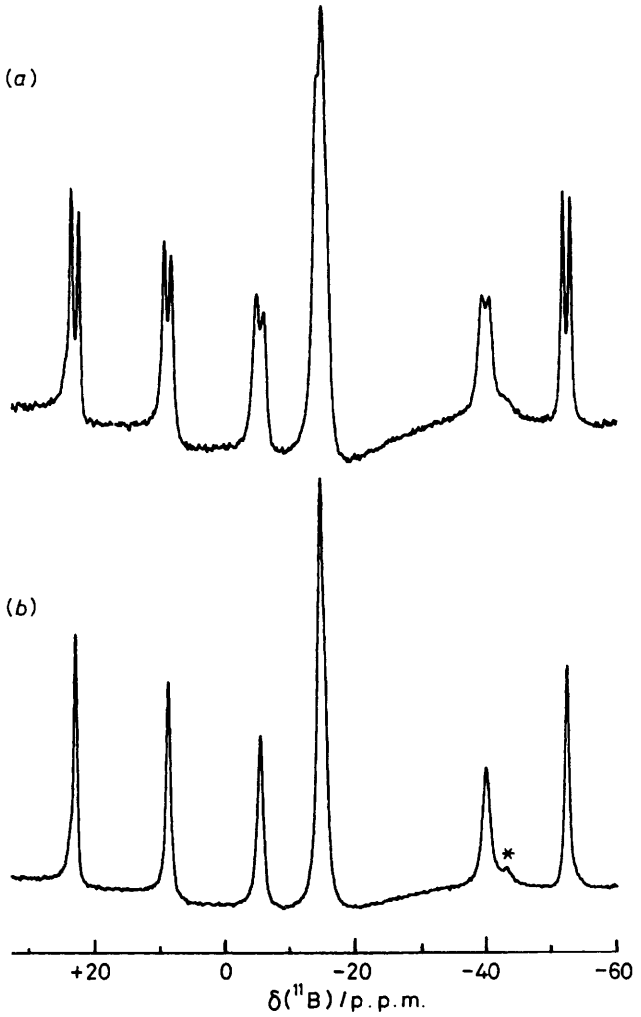

Figure 5. (*a*) Boron-11 and (*b*) ^{11}B-$\{^1H$(broad-band noise)$\}$ n.m.r. spectra (128 MHz) of *nido*-$[(CO)(PMe_3)_2IrB_8H_{11}]$ (4). The overall appearance is quite different to that of the *nido*-$[B_9H_{12}]^-$ anion (Table 7). * Signifies impurity

borane *arachno*-B_8H_{14}. In cluster bonding terms, the iridium centre $Ir(CO)(PMe_3)_2$ is isoelectronic and 'isolobal' with the boron(III) centre B·L, where L is a two-electron donor ligand, and the nine-vertex metallaborane cluster electronic structure is equivalent to the *nido* species $B_9H_{11}{\cdot}L$, or $[B_9H_{12}]^-$ (*i.e.* $L{\equiv}H^-$) of effective 3530 *styx* bonding topology.

There are few further points worthy of note concerning the n.m.r. data (Tables 5 and 6), as the impossibility of a complete assignment to cluster positions inhibits a useful discussion. {It may be noted that Table 5 also contains data for $[(PMe_3)_3IrB_{10}H_{11}]$ (6) which we were able to obtain by the thermolysis of a small quantity of *arachno*-$[(PMe_3)_3HIrB_8H_{12}]$ whilst in the pole gap of the n.m.r. magnet.} The mechanistic considerations below indicate that the chlorine substituent is on B(3) in the chloro-species (5) and the known [11,12] deshielding effect of *ca.* 15 p.p.m. on boron nuclear shielding in metallaborane systems when a hydrogen substituent is replaced by chlorine suggests that one of the resonances at $\delta(^{11}B)$ = *ca.* −14 p.p.m., probably that at −15.30, corresponds to B(3) in the non-chlorinated species (4). Interestingly, as mentioned above, there is no apparent large coupling $^3J(P{-}Ir{-}B{-}H)$ to H(3) in (4),

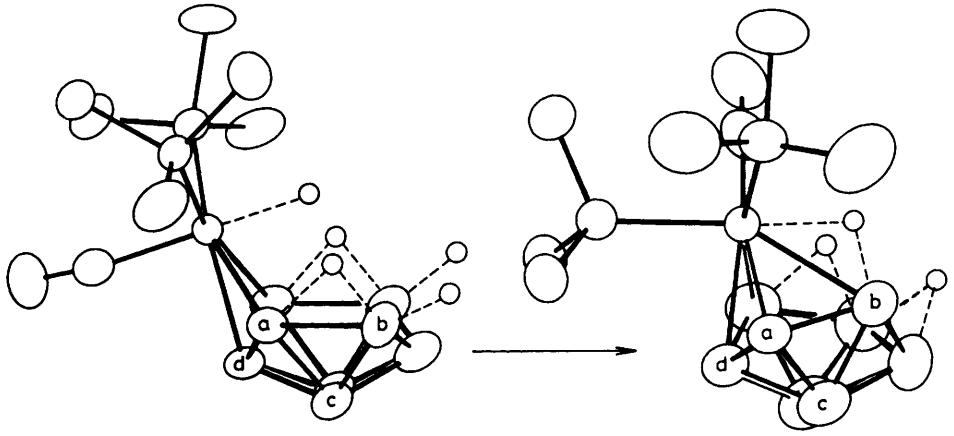

Figure 6. Adapted ORTEP drawings of the principal cluster atoms of the *arachno*-iridanonaboranes (1) and (2) (data from ref. 1) and the *nido*-iridanonaboranes (4) and (5), with bridging and *endo*-terminal hydrogen atoms added, to illustrate the probable geometry of the *arachno* ⟶ *nido* cluster closure process. Compound (1) has a chloro-substituent on the 1-position, atom (d), and it is reasonable to presume that it is also on the atom designated (d) in the product chloro-compound (5), *i.e.* in the 3-position

Table 8. First-order rate data for the quantitative thermal decomposition of *arachno*-$[(CO)(PMe_3)_2HIrB_8H_{11}Cl]$ (1) and *arachno*-$[(CO)(PMe_3)_2HIrB_8H_{12}]$ (2) in toluene solution to give *nido*-$[(CO)(PMe_3)_2IrB_8H_{10}Cl]$ (5) and *nido*-$[(CO)(PMe_3)_2IrB_8H_{11}]$ (4) respectively

(1) ⟶ (5)		(2) ⟶ (4)	
Temp. (°C)	$10^4k/s^{-1}$	Temp. (°C)	$10^4k/s^{-1}$
83	0.865		
86	1.73	90	1.08
90	3.07	95.5	1.40
94	5.16	101	4.37
97	5.86	110	8.06
101	9.01	110	8.10
101	10.21	110	8.31
104	10.06		
107	17.45		

$k[(1) \longrightarrow (5)] = [(8.7 \pm 1.0) \times 10^{13}]\exp\left[\frac{-(1.25 \pm 0.13) \times 10^5}{RT}\right] s^{-1}$ *

$k[(2) \longrightarrow (4)] = [(1.30 \pm 0.1) \times 10^{13}]\exp\left[\frac{-(1.30 \pm 0.06) \times 10^5}{RT}\right] s^{-1}$ *

* Error figures are the standard deviation, σ, in the *absolute* constants. Although in these terms the two processes have the same activation parameters within experimental error, the *relative* rates (1) ⟶ (5) and (2) ⟶ (4) are more accurately defined, *e.g.* at a given temperature in the range used (1) ⟶ (5) occurred some three times faster than (2) ⟶ (4).

in contrast to the *arachno* species (5),[1] and also in contrast to that observed for a similar geometric disposition in an Ir_2B_4 cluster species.[21] The selective sharpening of the Ir–H–B(5) bridging proton resonance in selective ^1H-$\{^{11}B\}$ experiments assigns B(5) in both compounds, and similarly the apparent selective sharpening of the B(6)–H–B(9) and B(8)–H–B(9) protons in this region assigns the other two associated boron nuclei to two of B(6), B(8) and B(9), but little can be said at present about other assignments. The overall shielding pattern for ^{11}B appears to be considerably different to that [36] for the parent $[B_9H_{12}]^-$ molecule (see Table 7). This is in contrast, for example, to that [20] for the *nido* ten-vertex iridium(III) species $[(PMe_3)_2HIrB_9H_{13}]$ which is quite closely related to that of $B_{10}H_{14}$, and also contrasts to that [1] of the *arachno* species $[(CO)(PMe_3)_2HIrB_8H_{12}]$ (2) which is closely related to that of $B_9H_{13}L$ and $[B_9H_{14}]^-$. However, although some tentative conclusions may be made by consideration of published evidence,[36] these are at best speculative at present and the spectrum of $[B_9H_{12}]^-$ itself (Table 7) also remains as yet unassigned; indeed the generally accepted structure for $[B_9H_{12}]^-$ has not been confirmed crystallographically.

The differences between the ^{11}B spectra of the *nido* compounds (4) and (5) (*e.g.* Figure 5) and the spectra [1] of their respective *arachno* precursors (2) and (1) permit certain individual resonances of both species to be well resolved in each case in the 32-MHz ^{11}B-$\{^1H$(broad-band noise)$\}$ n.m.r. spectrum. This enables the thermal decomposition (iii) to be followed conveniently by integrated n.m.r. spectroscopy, and using this technique it was found that at intermediate temperatures (80—110 °C) in toluene solution the reaction proceeds quantitatively with first-order kinetics. Typical rate constants thus determined at various temperatures are given in Table 8. The chloro-substituted compound (1) decomposed marginally the faster, and the rate data gave activation parameter values of $\Delta H^{\ddagger} = 122 \pm 13$ kJ mol^{-1} and $\Delta S^{\ddagger} = 29 \pm 7$ J K^{-1} mol^{-1} for the decomposition of (1) to give the chlorinated *nido* species (5), and 127 ± 6 kJ mol^{-1} and 29.5 ± 3 J K^{-1} mol^{-1} for the decomposition of (2) to give compound (4). These figures would tend to indicate that (*a*) the steric requirements for the transition state in both compound (1) and compound (2) are very similar, which is expected since the molecules differ in constitution only in substitution at B(1) which would not offer significant non-bonded interaction at the reacting centre (see below), but that (*b*) the electronegative chlorine atom stabilizes the transition state more effectively than hydrogen, presumably *via* cluster electronic effects.

The elimination of dihydrogen to form the *nido* species is clearly favoured; the reaction also takes place under mild u.v. irradiation, and also apparently for the positive molecular ion under electron impact in the mass spectrometer, as mentioned above and in ref. 1. The most plausible route would seem to be a closure of the *arachno* cage between Ir(4) and B(5) [*arachno* cage numbering system; [1] atom (b) in Figure 6] to give the Ir(2)–B(5) link of the *nido* species; this is illustrated in Figure 6. However, similar ligand geometries in (4) and (5) derive from different precursor geometries [(1) and (2)] and it is therefore necessary to postulate (in the transition state) a rotation of the metal vertex with respect to the borane cage.

Table 9. Fractional atomic co-ordinates for *nido*-[(CO)$(PMe_3)_2IrB_8H_{11}$] (4)

Atom	*X/a*	*Y/b*	*Z/c*	Atom	*X/a*	*Y/b*	*Z/c*
B(1)	−0.0592	0.0812	0.2114	C(3)	0.3721	0.2831	0.2373
Ir(2)	−0.004 27	0.258 39	0.190 32	H(31)	0.3555	0.2310	0.2883
B(3)	0.0621	0.1307	0.2891	H(32)	0.3599	0.3714	0.2526
B(4)	−0.1092	0.0652	0.3046	H(33)	0.4808	0.2690	0.2182
B(5)	−0.2202	0.1530	0.2358	C(4)	−0.2859	0.1808	0.0492
B(6)	0.0486	0.2772	0.3260	H(41)	−0.3568	0.2213	0.0891
B(7)	−0.0280	0.1637	0.3777	H(42)	−0.2791	0.0912	0.0623
B(8)	−0.2223	0.1771	0.3452	H(43)	−0.3297	0.1926	−0.0110
B(9)	−0.1091	0.2982	0.3805	C(5)	−0.1359	0.3739	0.0089
P(1)	0.2378	0.2467	0.1587	H(51)	−0.1928	0.4317	0.0465
P(2)	−0.1079	0.2415	0.0597	H(52)	−0.2000	0.3606	−0.0452
C(1)	0.2885	0.3436	0.0833	H(53)	−0.0310	0.4093	−0.0021
H(11)	0.2166	0.3316	0.0309	C(6)	−0.0143	0.1609	−0.0103
H(12)	0.4001	0.3274	0.0695	H(61)	0.0978	0.1893	−0.0099
H(13)	0.2792	0.4298	0.1039	H(62)	−0.0673	0.1733	−0.0685
C(2)	0.2949	0.1086	0.1271	H(63)	−0.0166	0.0719	0.0048
H(21)	0.2210	0.0787	0.0794	C(7)	0.0121	0.4200	0.1881
H(22)	0.2939	0.0503	0.1763	O(7)	0.0282	0.5174	0.1902
H(23)	0.4043	0.1139	0.1073				

Presumably the observed arrangement in the *nido* products represents the minimum-energy configuration. In steric terms the phosphines are in the least crowded positions with the smaller carbonyl group over the open face of the cluster. It may again be noted that on the present evidence it is not feasible to assign the position of the chlorine substituent in compound (5) with certainty and the possibility of an effective chlorine migration *via* cluster isomerizations cannot be rigorously excluded at this stage.

Only one other similar example of this type of elimination is known, *viz.* in the also facile and quantitative thermal dihydrogen elimination undergone by species such as [$(PMe_3)_2$-$HIrB_9H_{13}$],[22] and in this and the present case the starting compounds both have open-face bridging H atoms and an iridium(III) centre. The stability of the iridium(V) valency state is now well documented in these types of system,[18,22-25,27] and a reasonable mechanistic process could therefore be postulated in which there is an initial internal oxidative addition of the iridium(III) centre to the B–H–B bridge bond at atom (b). This would be followed by a reductive elimination of dihydrogen around the metal centre accompanied by an intra-cluster electronic rearrangement to form the product.

Experimental

General.—The *arachno*-metallaboranes [(CO)$(PMe_3)_2$-$HIrB_8H_{11}Cl$] (1) and [(CO)$(PMe_3)_2HIrB_8H_{12}$] (2) were synthesized as described elsewhere.[1] Reactions were carried out, and solids and solutions generally stored, under dry nitrogen, although manipulations and separatory procedures were generally carried out in air. Solvents were distilled from CaH_2 before use. Preparative and analytical thin-layer chromatography (t.l.c.) were carried out using silica-gel G with a fluorescence indicator (Fluka type GF254) as the stationary phase, using general procedures described in more detail in previous reports from these laboratories.[1,7,8,37] I.r. spectra were recorded on a Perkin-Elmer 457 instrument and values quoted are ±10 cm^{-1}. Mass spectra were recorded using an AEI/Kratos double-beam MS30 instrument using electron-impact ionization at 70 eV.

N.M.R. Spectroscopy.—The ^1H (100 MHz), ^{31}P (40 MHz), and ^{11}B (32 MHz) n.m.r. spectra were obtained using a JEOL FX100 instrument. ^{31}P-{^1H(broad-band noise)} spectra were recorded at lower temperatures to maximize line-sharpening arising from the 'thermal decoupling' of the effects of boron nuclear spins.[3] Selective ^1H-{^{11}B} double-resonance methods have been described elsewhere;[6,7,38,39] power levels used for these experiments were of the order of $\gamma B_2(^{11}B)/2\pi$ = 400 Hz, this value being estimated on the basis of off-resonance residual splittings as described elsewhere.[40] Temperature calibration was done by standard techniques and is considered accurate to within ±1.5 °C. Boron-11 (128 MHz) n.m.r. spectroscopy was carried out using the S.E.R.C. Bruker WH400 instrument at the University of Sheffield. Boron-11 and ^{31}P chemical shifts are quoted to high frequency (low field) of BF_3·OEt_2 in $CDCl_3$ (Ξ = 32 083 971 Hz)[39] and of 85% H_3PO_4 (Ξ = 40 480 730 Hz) respectively. Incidental to this work for purposes of comparison we have recorded the ^{11}B n.m.r. spectrum, and the ^1H-{^{11}B} n.m.r. spectra, of $[B_9H_{12}]^-$ at various temperatures; the proton shielding behaviour has not been reported previously and is summarized in Table 7. It is apparent that the molecule is fluxional with respect to bridging hydrogen site exchange, with ΔG *ca.* 52 kJ mol^{-1} at 279 K. The ΔG value was obtained using the coalescence temperature and the 2 : 1 site-exchange expression as described in ref. 41. It is of interest that the unique bridging H atom, observable at low temperatures, has a very high-field chemical shift for a B–H–B environment, which emphasizes the need for structural studies and spectroscopic assignment in this area of binary boron hydride chemistry.

Preparation of arachno-[(CO)$(PMe_3)_2HIrB_8H_{10}Pt(PMe_3)_2$] (3).—To a stirred solution of compound (2) (80 mg, 0.17 mmol) in tetrahydrofuran–CH_2Cl_2 (1 : 1, 20 cm^3) was added KH (20 mg, 0.5 mmol, 70% active). After *ca.* 15 min hydrogen evolution stopped and the mixture changed from colourless to pale yellow. [$PtCl_2(PMe_3)_2$] was then added and stirring continued for 1 h. The mixture was then filtered, reduced in volume (1—2 cm^3) and applied to a preparative t.l.c. plate using CH_2Cl_2–light petroleum (b.p. 40—60 °C) (4 : 1) as mobile phase. Many faint bands appeared on the plate under visible and u.v. illumination with just one main band showing under u.v. light at R_f = 0.4. This was rechromatographed until pure compound (3) (17 mg, 12% yield) was obtained. Colourless single crystals [$\nu_{max.}$(CO) = 2 000 cm^{-1}] were grown by

diffusion of pentane into a solution of (3) in CH_2Cl_2. These crystals decomposed in the *X*-ray beam of the diffractometer.

Preparation of nido-$[(CO)(PMe_3)_2IrB_8H_{11}]$ (4) *and nido*-$[(CO)(PMe_3)_2IrB_8H_{10}Cl]$ (5).—Compound (2) (11 mg, 0.02 mmol) was placed in a glass tube and the tube purged with nitrogen then sealed. It was then immersed in an oil bath maintained at 180 °C until the contents melted whereupon they turned red. The sample was dissolved in CH_2Cl_2, filtered, and applied to a preparative t.l.c. plate using CH_2Cl_2–light petroleum (b.p. 40—60 °C) (4 : 1) as mobile phase. This gave two main bands when viewed under u.v. light. They were the unreacted compound (2), $R_f = 0.8$ (2.6 mg), and *nido*-$[(CO)(PMe_3)_2IrB_8H_{11}]$ (4), $R_f = 0.6$ (6.6 mg, *ca.* 80% yield based on material reacted).

The product may also be produced by pentane diffusion into the n.m.r. sample used in the reaction rate experiments, giving very pale yellow crystals. Compound (5) is in fact best produced by this method as strong heating causes further decomposition.

X-*Ray Diffraction Analysis*.—A sample of [2,2,2-(CO)-$(PMe_3)_2$-*nido*-2-IrB_8H_{11}] was recrystallized from CH_2Cl_2–pentane yielding very pale yellow crystals suitable for single-crystal *X*-ray diffraction analysis. This diffraction work has been reported adequately in a preliminary communication,[27] but for convenience the data are summarized here. Crystals were monoclinic, space group $P2_1/n$, with $a = 916.0(3)$, $b = 1\,179.2(3)$, $c = 1\,695.5(3)$ pm, and $\beta = 93.81(2)°$. The structure was refined to $R = 0.032$ with anisotropic thermal parameters for non-hydrogen atoms, and with methyl H atoms included as part of rigid methyl groups (C–H = 108 pm) and $U_{iso} = 700$ pm^2. Atomic co-ordinates are given in Table 9.

Acknowledgements

We thank the S.E.R.C. for support and for a maintenance grant (to J. B.), and Dr. W. S. McDonald for very helpful collaboration in the *X*-ray diffraction experiments (ref. 27).

References

1 J. Bould, J. E. Crook, N. N. Greenwood, and J. D. Kennedy, *J. Chem. Soc., Dalton Trans.*, 1984, 1903.
2 N. N. Greenwood, J. D. Kennedy, and J. Staves, *J. Chem. Soc., Dalton Trans.*, 1978, 1146.
3 J. D. Kennedy and J. Staves, *Z. Naturforsch., Teil B*, 1979, **34**, 808.
4 N. N. Greenwood, M. J. Hails, J. D. Kennedy, and W. S. McDonald, *J. Chem. Soc., Chem. Commun.*, 1980, 37.
5 S. K. Boocock, N. N. Greenwood, and J. D. Kennedy, *J. Chem. Soc., Chem. Commun.*, 1980, 305.
6 J. D. Kennedy and B. Wrackmeyer, *J. Magn. Reson.*, 1980, **38**, 529.
7 S. K. Boocock, N. N. Greenwood, M. J. Hails, J. D. Kennedy, and W. S. McDonald, *J. Chem. Soc., Dalton Trans.*, 1981, 1415,
8 S. K. Boocock, N. N. Greenwood, J. D. Kennedy, W. S. McDonald, and J. Staves, *J. Chem. Soc., Dalton Trans.*, 1981, 2573.
9 Y. M. Cheek, N. N. Greenwood, J. D. Kennedy, and W. S. McDonald, *J. Chem. Soc., Chem. Commun.*, 1982, 80.
10 M. A. Beckett, J. E. Crook, N. N. Greenwood, J. D. Kennedy, and W. S. McDonald, *J. Chem. Soc., Chem. Commun.*, 1982, 552.
11 J. E. Crook, N. N. Greenwood, J. D. Kennedy, and W. S. McDonald, following paper; see also J. E. Crook, Ph.D. Thesis, University of Leeds, 1982.
12 R. Ahmad, N. N. Greenwood, and J. D. Kennedy, unpublished work; see also R. Ahmad, Ph.D. Thesis, University of Leeds, 1982.
13 N. N. Greenwood, M. J. Hails, J. D. Kennedy, and W. S. McDonald, *J. Chem. Soc., Dalton Trans.*, in the press; see also M. J. Hails, Ph.D. Thesis, University of Leeds, 1981.
14 N. N. Greenwood, *Pure Appl. Chem.*, 1977, **49**, 791.
15 J. D. Kennedy, Proc. 19th Int. Conf. Coord. Chem., Prague, 1978, vol. 1, p. 79.
16 N. N. Greenwood, J. D. Kennedy, W. S. McDonald, D. Reed, and J. Staves, *J. Chem. Soc., Dalton Trans.*, 1979, 117.
17 N. N. Greenwood, J. D. Kennedy, and D. Reed, *J. Chem. Soc., Dalton Trans.*, 1980, 196.
18 J. E. Crook, N. N. Greenwood, J. D. Kennedy, and W. S. McDonald, *J. Chem. Soc., Chem. Commun.*, 1981, 933.
19 J. Bould, N. N. Greenwood, and J. D. Kennedy, *J. Chem. Soc., Dalton Trans.*, 1982, 481.
20 S. K. Boocock, J. Bould, N. N. Greenwood, J. D. Kennedy, and W. S. McDonald, *J. Chem. Soc., Dalton Trans.*, 1982, 713.
21 J. E. Crook, N. N. Greenwood, J. D. Kennedy, and W. S. McDonald, *J. Chem. Soc., Chem. Commun.*, 1982, 383.
22 J. Bould, N. N. Greenwood, J. D. Kennedy, and W. S. McDonald, *J. Chem. Soc., Chem., Commun.*, 1982, 465.
23 J. Crook, N. N. Greenwood, J. D. Kennedy, and W. S. McDonald, *J. Chem. Soc., Chem. Commun.*, 1983, 83.
24 J. Bould, N. N. Greenwood, J. D. Kennedy, and W. S. McDonald, *J. Chem. Soc., Dalton Trans.*, submitted for publication.
25 J. Bould, N. N. Greenwood, and J. D. Kennedy, *J. Organomet. Chem.*, 1983, **249**, 11.
26 M. A. Beckett, J. E. Crook, N. N. Greenwood, and J. D. Kennedy, *J. Chem. Soc., Dalton Trans.*, 1984, 1427.
27 J. Bould, J. E. Crook, N. N. Greenwood, J. D. Kennedy, and W. S. McDonald, *J. Chem. Soc., Chem. Commun.*, 1982, 346.
28 T. L. Venable and R. N. Grimes, *Inorg. Chem.*, 1982, **21**, 887.
29 T. L. Venable, E. Sinn, and R. N. Grimes, *Inorg. Chem.*, 1982, **21**, 895.
30 R. Ahmad, J. E. Crook, N. N. Greenwood, J. D. Kennedy, and W. S. McDonald, *J. Chem. Soc., Chem., Commun.*, 1982, 1019.
31 K. R. Dixon, M. Fakley, and A. Pidcock, *Can. J. Chem.*, 1976, **54**, 2733.
32 J. C. Huffman and W. E. Streib, *J. Chem. Soc., Chem. Commun.*, 1972, 665.
33 M. Green, J. L. Spencer, F. G. A. Stone, and A. Welch, *J. Chem. Soc., Chem. Commun.*, 1974, 794.
34 C. H. Schwalbe and W. N. Lipscomb, *Inorg. Chem.*, 1971, **10**, 160.
35 J. Dobson and R. Schaeffer, *Inorg. Chem.*, 1968, **7**, 402.
36 A. R. Siedle, G. M. Bodner, A. R. Garber, and L. J. Todd, *Inorg. Chem.*, 1974, **13**, 1756.
37 S. K. Boocock, N. N. Greenwood, J. D. Kennedy, W. S. McDonald, and J. Staves, *J. Chem. Soc., Dalton Trans.*, 1980, 790.
38 J. D. Kennedy and N. N. Greenwood, *Inorg. Chim. Acta*, 1980, **38**, 93.
39 J. D. Kennedy, 'Boron,' ch. 8 in 'NMR in Organometallic and Inorganic Chemistry,' ed. J. Mason, Plenum, in the press.
40 T. C. Gibb and J. D. Kennedy, *J. Chem. Soc., Faraday Trans. 2*, 1982, 525.
41 J. Bould and B. J. Brisdon, *Inorg. Chim. Acta*, 1976, **19**, 159.

Received 12*th December* 1983; *Paper* 3/2192